714 *Inorg. Chem.* **2010**, *49*, 714–720
DOI: 10.1021/ic9020349

Inorganic Chemistry
Article

Cyanide Anion Binding by a Triarylborane at the Outer Rim of a Cyclometalated Ruthenium(II) Cationic Complex

Casey R. Wade and François P. Gabbaï*

Department of Chemistry, Texas A&M University, College Station, Texas 77843

Received October 14, 2009

As part of our ongoing interest in the design of boron-based cyanide anion receptors, we have synthesized a triaryl borane decorated by a cationic Ru(II) complex and have investigated its anion binding properties. This new borane, [(2,2′-bpy)Ru(κ-*C*,*N*-2-(dimesitylborylphenyl)pyridinato)]OTf ([**2**]OTf), binds both fluoride and cyanide anions in organic solvents to afford **2**-F and **2**-CN whose crystal structures have been determined. UV−vis titrations in 9/1 $CHCl_3$/DMF (vol.) afforded $K_{(F^-)} = 1.1(\pm 0.1) \times 10^4\ M^{-1}$ and $K_{(CN^-)} = 3.0(\pm 1.0) \times 10^6\ M^{-1}$ indicating that $[\mathbf{2}]^+$ has a higher affinity for cyanide than for fluoride in this solvent mixture. These elevated binding constants show that the cationic Ru(II) complex increases the anion affinity of these complexes via Coulombic and inductive effects. The UV−vis spectral changes which accompany either fluoride or cyanide binding to the boron center are similar and include a 30 nm bathochromic shift of the metal-to-ligand charge transfer band. This shift is attributed to an increase in the donor ability of the boron-substituted phenylpyridine ligand upon anion binding to the boron center. Accordingly, cyclic voltammetry revealed that the $Ru^{II/III}$ redox couple of [**2**]OTf ($E_{1/2} = +0.051$ V vs Fc/Fc^+) undergoes a cathodic shift upon F^- ($\Delta E_{1/2} = -0.242$ V vs Fc/Fc^+) or CN^- ($\Delta E_{1/2} = -0.198$ V vs Fc/Fc^+) binding.

Introduction

Triaryl boranes are receiving a great deal of interest as receptors for small nucleophilic anions[1] including the highly toxic cyanide anion.[2−5] The validity of this approach can be illustrated by the ability of the cationic boranes $[\mathbf{I}]^+$ and $[\mathbf{II}]^+$ to complex cyanide anions in neutral water at concentrations as low as 50 ppb.[3] These unusual properties can be assigned to the presence of the cationic group which inductively enhances the electron deficiency of the boron center while providing a Coulombic drive for the complexation of the anion.[6,7]

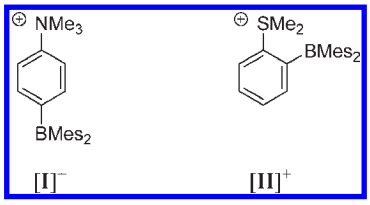

In parallel to these developments, an increasing amount of attention has been devoted to the synthesis and anion binding properties of boron derivatives containing a transition metal moiety.[5,8−10] The study of such compounds has been

*To whom correspondence should be addressed. E-mail: francois@tamu.edu.

(1) Hudnall, T. W.; Chiu, C.-W.; Gabbaï, F. P. *Acc. Chem. Res.* **2009**, *42*, 388–397. Yamaguchi, S.; Wakamiya, A. *Pure Appl. Chem.* **2006**, *78*, 1413–1424.

(2) Parab, K.; Venkatasubbaiah, K.; Jäkle, F. *J. Am. Chem. Soc.* **2006**, *128*, 12879–12885. Parab, K.; Venkatasubbaiah, K.; Qin, Y.; Jäkle, F. *Polym. Prepr.* **2007**, *48*, 699–700. Chiu, C.-W.; Kim, Y.; Gabbaï, F. P. *J. Am. Chem. Soc.* **2009**, *131*, 60–61. Agou, T.; Sekine, M.; Kobayashi, J.; Kawashima, T. *Chem.—Eur. J.* **2009**, *15*, 5056–5062.

(3) Hudnall, T. W.; Gabbaï, F. P. *J. Am. Chem. Soc.* **2007**, *129*, 11978–11986. Kim, Y.; Zhao, H.; Gabbaï, F. P. *Angew. Chem., Int. Ed.* **2009**, *48*, 4957–4960.

(4) Chiu, C.-W.; Gabbaï, F. P. *Dalton Trans.* **2008**, 814–817. Huh, J. O.; Do, Y.; Lee, M. H. *Organometallics* **2008**, *27*, 1022–1025.

(5) Broomsgrove, A. E. J.; Addy, D. A.; Bresner, C.; Fallis, I. A.; Thompson, A. L.; Aldridge, S. *Chem.—Eur. J.* **2008**, *14*, 7525–7529.

(6) Agou, T.; Kobayashi, J.; Kawashima, T. *Inorg. Chem.* **2006**, *45*, 9137–9144. Chiu, C.-W.; Gabbaï, F. P. *J. Am. Chem. Soc.* **2006**, *128*, 14248–14249. Agou, T.; Kobayashi, J.; Kim, Y.; Gabbaï, F. P.; Kawashima, T. *Chem. Lett.* **2007**, *36*, 976–977. Hudnall, T. W.; Kim, Y.-M.; Bebbington, M. W. P.; Bourissou, D.; Gabbaï, F. P. *J. Am. Chem. Soc.* **2008**, *130*, 10890–10891. Kim, Y.; Hudnall, T. W.; Bouhadir, G.; Bourissou, D.; Gabbaï, F. P. *Chem. Commun.* **2009**, 3729–3731.

(7) Lee, M. H.; Agou, T.; Kobayashi, J.; Kawashima, T.; Gabbaï, F. P. *Chem. Commun.* **2007**, 1133–1135.

(8) Sakuda, E.; Funahashi, A.; Kitamura, N. *Inorg. Chem.* **2006**, *45*, 10670–10677. Sun, Y.; Ross, N.; Zhao, S. B.; Huszarik, K.; Jia, W. L.; Wang, R. Y.; Macartney, D.; Wang, S. *J. Am. Chem. Soc.* **2007**, *129*, 7510–7511. Zhao, S.-B.; McCormick, T.; Wang, S. *Inorg. Chem.* **2007**, *46*, 10965–10967. Zhao, Q.; Li, F.; Liu, S.; Yu, M.; Liu, Z.; Yi, T.; Huang, C. *Inorg. Chem.* **2008**, *47*, 9256–9264.

(9) Boshra, R.; Venkatasubbaiah, K.; Doshi, A.; Lalancette, R. A.; Kakalis, L.; Jäkle, F. *Inorg. Chem.* **2007**, *46*, 10174–10186. Day, J. K.; Bresner, C.; Coombs, N. D.; Fallis, I. A.; Ooi, L.-L.; Aldridge, S. *Inorg. Chem.* **2008**, *47*, 793–804. You, Y.; Park, S. Y. *Adv. Mater.* **2008**, *20*, 3820–3826. Hudson, Z. M.; Zhao, S.-B.; Wang, R.-Y.; Wang, S. *Chem.—Eur. J.* **2009**, *15*, 6131–6137. Lam, S.-T.; Zhu, N.; Yam, V. W.-W. *Inorg. Chem.* **2009**, *48*(20), 9664–9670. Parab, K.; Jäkle, F. *Macromolecules* **2009**, *42*, 4002–4007. Sun, Y.; Wang, S. *Inorg. Chem.* **2009**, *48*, 3755–3767. Aldridge, S.; Bresner, C.; Fallis, I. A.; Coles, S. J.; Hursthouse, M. B. *Chem. Commun.* **2002**, 740–741. Bresner, C.; Aldridge, S.; Fallis, I. A.; Jones, C.; Ooi, L.-L. *Angew. Chem., Int. Ed.* **2005**, *44*, 3606–3609. Coombs, N. D.; Aldridge, S.; Wiltshire, G.; Kays, D. L.; Bresner, C.; Ooi, L.-l. *J. Organomet. Chem.* **2005**, *690*, 2725–2731. Bresner, C.; Day, J. K.; Coombs, N. D.; Fallis, I. A.; Aldridge, S.; Coles, S. J.; Hursthouse, M. B. *Dalton Trans.* **2006**, 3660–3667.

Published on Web 12/11/2009

motivated by the unusual physicochemical properties imparted by the presence of the transition metal and their response to anion binding at the boron center. Examples of such compounds include **III** whose oxidation potential undergoes a cathodic shift of 560 mV upon binding of cyanide to the boron center.[5] Interestingly, relatively little effort has been devoted to the study of cationic transition metal/boron derivatives as anion receptors. Anticipating the occurrence of favorable Coulombic and inductive effects, we have set out to synthesize examples of such compounds and probe their affinity toward cyanide among other anions. Prior efforts in this area of chemistry have yielded derivatives such as $[\mathbf{IV}]^+$–$[\mathbf{VII}]^+$.[8] Although such derivatives have been well characterized, relatively little is known about their affinity for anions other than fluoride, and the structures of the fluoride adducts remain unknown.

Targeting the cyanide anion as an analyte, we decided to focus on a robust complex whose transition metal center would not react with the cyanide ligand. In this paper, we report a series of results that we have obtained on the synthesis and study of such a compound.

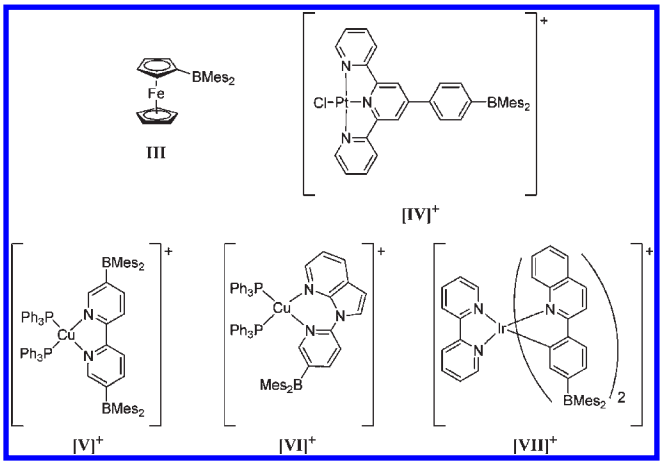

Experimental Section

General Considerations. 2-(4′-Dimesitylborylphenyl)pyridine was synthesized by a published procedure.[11] Dimesitylboron fluoride (Mes_2BF) and tetraethylammonium cyanide (TEACN) were purchased from Aldrich. *n*-$Bu_4NF\cdot 3H_2O$ (TBAF) was purchased from Alfa Aesar and used as received. Solvents were dried by passing through an alumina column (*n*-hexane, CH_2Cl_2) or refluxing under N_2 over Na/K (Et_2O and tetrahydrofuran (THF)). Air-sensitive compounds were handled under a N_2 atmosphere using standard Schlenk and glovebox techniques. UV–vis spectra were recorded on either an HP8453 spectrophotometer or an Ocean Optics USB4000 spectrometer with an Ocean Optics ISS light source. Elemental analyses were performed at Atlantic Microlab (Norcross, GA). NMR spectra were recorded on Varian Unity Inova 400 FT NMR (399.59 MHz for ^{1}H, 375.99 MHz for ^{19}F, 128.19 MHz for ^{11}B, 100.45 MHz for ^{13}C) spectrometer at ambient temperature unless otherwise stated. Chemical shifts δ are given in parts per million, and are referenced against external Me_4Si (^{1}H, ^{13}C) and $BF_3\cdot Et_2O$ (^{11}B, ^{19}F).

Synthesis of [(2,2′-bpy)Ru(κ-*C*,*N*-2-(dimesitylborylphenyl)-pyridinato)]OTf ([2]OTf). AgOTf (0.102 g, 0.400 mmol) was added as a solid to a solution of $bpy_2RuCl_2\cdot 2H_2O$ (0.100 g, 0.2 mmol) and **1** (0.400 g, 1.00 mmol) in 3 mL of CH_2Cl_2 and 10 mL of MeOH. The mixture was heated to reflux for 2 h and the solvent removed in vacuo. The resulting purple solid was extracted with 20 mL of CH_2Cl_2 and filtered over Celite. The solvent was again removed, and the residue washed with 3 × 10 mL of Et_2O and 5 mL of cold acetonitrile. Recrystallization of the crude product by slow diffusion of Et_2O into a CH_2Cl_2 solution gave the pure product in 52% yield as dark purple needles. ^{1}H NMR (399.9 MHz, pyridine-d_5): δ 2.01 (s, 12H, Mes-CH_3), 2.31 (s, 6H, Mes-CH_3), 6.72 (s, 1H, Ph−C*H*), 6.81 (s, 4H, Mes-C*H*), 6.94 (t, $^3J_{H-H}$ = 7.08 Hz, 1H, Pyr-C*H*), 7 (t, $^3J_{H-H}$ = 7.14 Hz, 1H, Pyr-C*H*), 7.05–7.09 (m, 2H, Pyr-C*H*), 7.34 (d, $^3J_{H-H}$ = 7.88 Hz, 1H, Pyr-C*H*), 7.40 (t, $^3J_{H-H}$ = 6.41 Hz, 1H, Pyr-C*H*), 7.54 (t, $^3J_{H-H}$ = 8.06 Hz, 1H, Pyr-C*H*), 7.58 (t, $^3J_{H-H}$ = 7.33 Hz, 1H, Pyr-C*H*), 7.65 (t, $^3J_{H-H}$ = 8.06 Hz, 1H, Pyr-C*H*), 7.68 (d, $^3J_{H-H}$ = 7.68 Hz, 1H, Pyr-C*H*), 7.72 (d, $^3J_{H-H}$ = 6.04 Hz 1H, Pyr-C*H*), 7.82 (d, $^3J_{H-H}$ = 5.67 Hz 1H, Pyr-C*H*), 7.89 (d, $^3J_{H-H}$ = 8.24 Hz, 1H, Pyr-C*H*), 8.01 (d, $^3J_{H-H}$ = 5.67 Hz, 1H, Pyr-C*H*), 8.05 (d, $^3J_{H-H}$ = 7.87 Hz, 1H, Pyr-C*H*), 8.12 (d, $^3J_{H-H}$ = 5.31 Hz, 1H, Pyr-C*H*), 8.16 (d, $^3J_{H-H}$ = 8.24 Hz, 1H, Pyr-C*H*), 8.32–8.29 (m, 2H, Pyr-C*H*), 8.46 (d, $^3J_{H-H}$ = 8.42 Hz, 1H, Pyr-C*H*), 8.50 (d, $^3J_{H-H}$ = 7.69 Hz, 1H, Pyr-C*H*), 8.61 (d, $^3J_{H-H}$ = 8.24 Hz, 1H, Pyr-C*H*). ^{13}C NMR (100.5 MHz, acetone-d_6): δ 21.07 (Mes-*p*-CH_3), 23.25 (Mes-*o*-CH_3), 120.38, 123.50, 123.58, 123.70, 123.93, 124.04, 124.29, 126.59, 126.74, 126.88, 127.89, 128.54, 128.91, 133.94, 134.28, 135.65, 136.44, 137.07, 138.53, 140.70, 142.87, 144.01, 150.00, 150.02, 150.12, 150.84, 151.12, 154.87, 155.96, 157.25, 157.61, 158.63, 167.92, 183.91, 192.04 (Ph-*C*-Ru). ^{11}B NMR (128.2 MHz, CD_2Cl_2): δ 74. Anal. Calcd for $C_{50}H_{45}BF_3N_5O_3SRu$: C, 62.24; H, 4.70; N, 7.26. Found: C, 62.15; H, 4.67; N, 7.24.

Generation of 2-F and 2-CN. **2**-F and **2**-CN were prepared and characterized by multinuclear NMR in situ by addition of a slight excess of TBAF or TEACN, respectively, to solutions of [**2**]OTf in pyridine-d_5. or acetone- d_6. Data for **2**-CN: ^{1}H NMR (399.9 MHz, pyridine-d_5): δ 2.14 (s, 6H, Mes-CH_3), 2.24 (s, 3H, Mes-CH_3), 2.29 (s, 3H, Mes-CH_3), 2.45 (s, 6H, Mes-CH_3), 6.53 (s, 1H, Ph−C*H*), 6.64 (s, 2H, Mes-C*H*), 6.68 (t, $^3J_{H-H}$ = 6.77 Hz, 1H, Pyr-C*H*), 6.75 (s, 2H, Mes-C*H*), 6.84–6.95 (m, 4H, Pyr-C*H*), 7.30 (d, $^3J_{H-H}$ = 7.14 Hz, 1H, Pyr-C*H*), 7.40 (d, $^3J_{H-H}$ = 7.14 Hz, 1H, Pyr-C*H*), 7.48–7.60 (m, 3H, Pyr-C*H*), 7.82–7.90 (m, 3H, Pyr-C*H*), 7.96 (m, 2H, Pyr-C*H*), 8.07 (m, 2H, Pyr-C*H*), 8.23 (d, 1H, Pyr-C*H*, $^3J_{H-H}$ = 8.06 Hz), 8.34 (d, 1H, Pyr-C*H*, $^3J_{H-H}$ = 7.69 Hz), 8.49 (d, 1H, Pyr-C*H*, $^3J_{H-H}$ = 78.24 Hz), 8.52 (d, 1H, Pyr-C*H*, $^3J_{H-H}$ = 5.5 Hz), 8.62 (d, 1H, Pyr-C*H*, $^3J_{H-H}$ = 8.06 Hz). ^{13}C NMR (100.5 MHz, pyridine-d_5): δ 21.09 (Mes-*p*-CH_3), 21.12 (Mes-*p*-CH_3), 25.84 (Mes-*o*-CH_3), 26.42 (Mes-*o*-CH_3), 118.04, 120.64, 122.69, 122.75, 123.03, 123.21, 125.56, 125.77, 125.84, 127.17, 129.24, 129.38, 130.93, 131.24, 131.44, 132.42, 133.18, 134.12, 135.27, 140.31, 142.67, 142.76, 143.67, 149.01, 149.12, 155.08, 156.76, 157.13, 158.02, 165.89, 169.50, 189.48 (Ph-*C*-Ru). ^{11}B NMR (128.2 MHz, pyridine-d_5): δ −12.7 Data for **2**-F: ^{1}H NMR (399.9 MHz, acetone- d_6): δ 1.28 (s, 3H, Mes-CH_3), 1.61 (s, 6H, Mes-CH_3), 1.89 (s, 6H, Mes-CH_3), 2.14 (s, 3H, Mes-CH_3), 6.13 (bs, 1H, Ph−C*H*), 6.26 (bs, 2H, Mes-C*H*), 6.33 (bs, 2H, Mes-C*H*), 6.75 (t, 1H, Pyr-C*H*, $^3J_{H-H}$ = 6.52 Hz), 6.94 (br, 1H, Pyr-C*H*), 7.15–7.21 (bm, 3H, Pyr-C*H*), 7.37 (br, 2H, Pyr-C*H*), 7.45 (d, 1H, Pyr-C*H*, $^3J_{H-H}$ = 5.50 Hz), 7.50 (d, 1H, Pyr-C*H*, $^3J_{H-H}$ = 6.4 Hz), 7.55 (t, 1H, Pyr-C*H*, $^3J_{H-H}$ = 7.60 Hz), 7.61 (t, 1H, Pyr-C*H*, $^3J_{H-H}$ = 7.62 Hz), 7.67 (t, 1H, Pyr-C*H*, $^3J_{H-H}$ = 6.8 Hz), 7.83–7.88 (m, 3H, Pyr-C*H*), 8.02–8.07 (m, 3H, Pyr-C*H*), 8.19 (br, 1H, Pyr-C*H*), 8.32 (br, 1H, Pyr-C*H*), 8.70 (d, 1H, Pyr-C*H*, $^3J_{H-H}$ = 8.26 Hz), 8.80 (d, 1H, Pyr-C*H*, $^3J_{H-H}$ = 8.26 Hz). ^{13}C NMR (100.5 MHz, pyridine-d_5): δ 21.27 (Mes-*p*-CH_3), 21.30 (Mes-*p*-CH_3) 25.82 (Mes-*o*-CH_3), 26.22

(10) Zhou, G.; Ho, C.-L.; Wong, W.-Y.; Wang, Q.; Ma, D.; Wang, L.; Lin, Z.; Marder, T. B.; Beeby, A. *Adv. Funct. Mater.* **2008**, *18*, 499–511. Rao, Y.-L.; Wang, S. *Inorg. Chem.* **2009**, *48*, 7698–7713.
(11) Wade, C. R.; Gabbaï, F. P. *Dalton Trans.* **2009**, 9169–9175.

(Mes-*o*-CH_3), 117.76, 120.18, 122.69, 122.75, 123.03, 123.12, 124.06, 125.46, 125.68, 125.92, 127.10, 128.79, 128.86, 130.48, 130.78, 132.22, 133.07, 133.98, 135.11, 139.69, 142.35, 148.91, 149.25, 149.37, 155.28, 155.70, 156.89, 157.14, 158.01, 168.60, 169.91, 188.98 (Ph-*C*-Ru). ^{19}F NMR (375.97 MHz, pyridine-d_5): δ −176.39 (90%), 176.19 (10%). Anal. Calcd for $C_{54}H_{50}BFN_6Ru$: C, 70.97; H, 5.51; N, 9.20. Found: C, 70.30; H, 5.43; N, 9.25.

Titration of [2]OTf with Fluoride and Cyanide in THF/DMF. Solutions of [**2**]OTf (3.0 mL, 2.5×10^{-5} M, 9/1 DMF/THF) were titrated with incremental (5 μL) amounts of fluoride or cyanide anions by addition of a 3.5×10^{-3} M solution of TBAF in DMF or a 3.0×10^{-3} M solution of TEACN in DMF.

Electrochemistry. Electrochemical experiments were performed with an electrochemical analyzer from CH Instruments (Model 610A) with a glassy carbon working electrode and a platinum auxiliary electrode. The reference electrode was built from a silver wire inserted in a small glass tube fitted with a porous vycor frit at the tip and filled with a THF solution containing (n-Bu)$_4$NPF$_6$ (0.1 M) and $AgNO_3$ (0.005 M). All three electrodes were immersed in a *N*,*N*-dimethylformamide (DMF) solution (3 mL) containing 0.1 M of supporting electrolyte ((n-Bu)$_4$NPF$_6$) and 0.001 M of [**2**]OTf. **2**-F and **2**-CN were prepared in situ in the electrochemical cell by addition of 0.1 mL of 0.03 M TEACN or TBAF solutions in DMF. In all cases, ferrocene was used as an internal standard, and all potentials are reported with respect to the $E_{1/2}$ of the Fc^+/Fc redox couple.

Crystallography. Single crystals of [**2**]OTf could be obtained by slow diffusion of Et_2O into a solution of the compound in CH_2Cl_2. Single crystals of **2**-F could be obtained by slow evaporation of a mixture of [**2**]OTf and TBAF in pyridine-d_5. Single crystals of **2**-CN were obtained by slow evaporation of a mixture of [**2**]OTf and KCN in 1/1 acetone/MeOH. The crystallographic measurement of [**2**]OTf, **2**-F, and **2**-CN were performed using a Bruker APEX-II CCD area detector diffractometer, with a graphite-monochromated Mo Kα radiation (λ = 0.71069 Å). A specimen of suitable size and quality was selected and mounted onto a nylon loop. The structure was solved by direct methods, which successfully located most of the non-hydrogen atoms. Subsequent refinement on F^2 using the SHELXTL/PC package (version 6.10) allowed location of the remaining non-hydrogen atoms.[12]

Theoretical Calculations. Density functional theory (DFT) calculations (full geometry optimization) were carried out on [**2**]$^+$, **2**-CN, and **2**-F starting from the crystal structure geometries with Gaussian03 utilizing the gradient-corrected Becke exchange functional (B3LYP) and the Lee−Yang−Parr correlation functional. A 6-31+g(d′) basis set was used for C, H, N, B, and F. A Stuttgart RSC 1997 ECP basis set was used for Ru. Frequency calculations were also carried out on the optimized geometry, showing no imaginary frequencies. Single point energy calculations were performed using the Polarizable Continuum Model (PCM) and THF as a solvent.

Results and Discussion

Coordinatively saturated cyclometalated ruthenium complexes such as [(2,2′-bpy)$_2$Ru(2-ppy)]$^+$ (2-ppy = κ-*C*,*N*-2-phenylpyridinato) have been previously studied and shown to possess a relatively inert core.[13−16] Moreover, such complexes possess well-understood electrochemical and photophysical properties.[13−16] Encouraged by these precedents, we decided to investigate the synthesis of a borylated analogue of such a complex. Consequently, the known 2-(4′-dimesitylborylphenyl)pyridine (**1**),[11] which has been incorporated in iridium and platinum complexes,[10] was allowed to react with (2,2′-bpy)$_2$RuCl$_2$ in refluxing CH_2Cl_2/MeOH in the presence of AgOTf (Scheme 1) to afford [**2**]OTf as dark purple needles in 52% yield after recrystallization from CH_2Cl_2/Et_2O.[16] Salt [**2**]OTf has been fully characterized, and its crystal structure determined. It displays moderate solubility in polar organic solvents such as THF, CH_2Cl_2, DMSO, acetone, and pyridine but is insoluble in H_2O and less polar solvents such as Et_2O and pentane. The ^{1}H NMR spectrum of [**2**]OTf (pyridine-d_5) displays distinct resonances for each of the aryl C*H* groups of the 2,2′-bpy and phenylpyridyl ligands. The presence of single mesityl aromatic C*H* and ortho- and meta-CH_3 resonances indicates equivalency of boron mesityl substituents at room temperature. The broad signal observed at 74 ppm in the ^{11}B NMR spectrum (CD_2Cl_2) is characteristic of a triarylborane.

Scheme 1

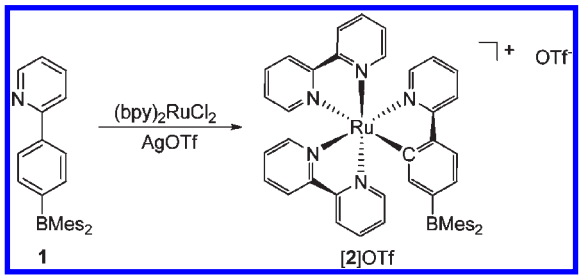

The UV−vis spectrum of [**2**]OTf (THF/DMF, 9/1 vol.) displays two prominent features: a sharp band at 335 nm (ε = 33 460), assigned to absorption of the triarylborane-based chromophore, and a broad metal-to-ligand-charge-transfer (MLCT) band with λ_{max} = 550 nm (ε = 11 650) spanning the 450−625 nm range. This MLCT band appears in the same range as that reported for the parent cation [(bpy)$_2$-Ru(2-ppy)]$^+$.[14] Cyclic voltammetry experiments performed on **2**[OTf] show that it undergoes a fully reversible $Ru^{II/III}$ redox couple at $E_{1/2}$ = +0.051 V versus Fc/Fc^+ (1 mM, 0.1 M $TBAPF_6$, DMF, glassy carbon electrode, 200 mV scan rate). To understand the effects, if any, of the pendant dimesitylboryl group on the $Ru^{II/III}$ redox couple, the cyclic voltammogram of the non-borylated complex, [(bpy)$_2$Ru-(2-ppy)]OTf, was recorded. Under the same conditions, this complex undergoes oxidation at $E_{1/2}$ = +0.025 V versus Fc/Fc^+, indicating that decoration of the phenylpyridyl ligand with a dimesitylboryl moiety has only a limited influence on the redox properties of the complex (Supporting Information, Figure S1).

The crystal structure of [**2**]OTf confirms the presence of the cyclometalated ligand bearing a dimesitylboryl group (Figure 1, Table 1). The Ru−N bond distances are all within the 2.035(4)−2.070(4) Å range, with the exception of the Ru(1)−N(5) bond trans to the Ru(1)−C(7) bond that is somewhat elongated (2.152(4) Å) because of the strong trans effect of the carbanionic ligand. The Ru(1)−C(7) bond was measured to be 2.038(5) Å, in the range of Ru−C distances

(12) Sheldrick, G. M. *SHELXTL/PC*, Version 6.10; Bruker AXS Inc.: Madison, WI, 1999.
(13) Reveco, P.; Schmehl, R. H.; Cherry, W. R.; Fronczek, F. R.; Selbin, J. *Inorg. Chem.* **1985**, *24*, 4078–4082.
(14) Constable, E. C.; Holmes, J. M. *J. Organomet. Chem.* **1986**, *301*, 203–208. Reveco, P.; Cherry, W. R.; Medley, J.; Garber, A.; Gale, R. J.; Selbin, J. *Inorg. Chem.* **1986**, *25*, 1842–1845.
(15) Constable, E. C.; Leese, T. A. *J. Organomet. Chem.* **1987**, *335*, 293–299. Constable, E. C.; Housecroft, C. E. *Polyhedron* **1990**, *9*, 1939–1947.
(16) Sasaki, I.; Vendier, L.; Sournia-Saquet, A.; Lacroix, P. G. *Eur. J. Inorg. Chem.* **2006**, 3294–3302.

Table 1. Crystal Data, Data Collections, and Structure Refinements

crystal data	**2**[OTf]	**2**-F	**2**-CN
formula	$C_{50}H_{45}BF_3N_5O_3SRu$	$C_{49}H_{45}BFN_5Ru-C_6H_5N$	$C_{50}H_{45}BN_6Ru-CH_3OH$
M_r	964.85	917.91	873.84
crystal size/mm	0.17 × 0.12 × 0.08	0.18 × 0.15 × 0.10	0.35 × 0.08 × 0.06
crystal system	monoclinic	monoclinic	tetragonal
space group	*P*2(1)/*c*	*P*2(1)/*c*	*P*4(3)
a/Å	14.3700(4)	14.003(4)	11.2355(10)
b/Å	21.1565(7)	23.236(7)	11.2355(10)
c/Å	14.8607(5)	16.816(4)	32.768(3)
β/deg	103.511(2)	128.800(15)	
V/Å^3	4392.9(2)	4381.2(19)	4136.5(6)
Z	4	4	4
ρ_{calc}/g cm^{-3}	1.459	1.392	1.392
μ/mm^{-1}	0.467	0.408	0.426
F(000)	1984	1912	1812
T/K	110(2)	110(2)	110(2)
scan mode	*ω*, *φ*	*ω*, *φ*	*ω*, *φ*
hkl range	−16 → +16	−16 → +16	−13 → +13
	−24 → +21	−26 → +26	−14 → +14
	−16 → +16	−19 → +19	−37 → +43
measd reflns	32052	45426	30058
unique reflns [R_{int}]	6657 [0.0585]	6856 [0.0888]	9663 [0.0836]
reflns used for refinement	6657	6856	9663
refined parameters	614	568	543
GoF	1.001	1.000	1.000
*R*1,[a] *wR*2[b] (all data)	0.0809, 0.1281	0.0908, 0.1715	0.0775, 0.1073
ρ_{fin} (max., min.)/e Å^{-3}	0.921, −1.111	2.051, −1.010	0.528, −0.576

[a] $R1 = \sum||F_o| - |F_c||/\sum|F_o|$. [b] $wR2 = [\sum w(F_o^2 - F_c^2)^2/\sum w(F_o^2)^2]^{1/2}$; $w = 1/[\sigma^2(F_o^2) + (ap)^2 + bp]$; $p = (F_o^2 + 2F_c^2)/3$ with $a = 0.0694$ for **[2]**OTf, 0.0710 for **2**-F, and 0.0362 for **2**-CN; and $b = 0$ for **[2]**OTf, 21 for **2**-F, and 0 for **2**-CN.

observed for similar complexes.[13,16,17] The boron atom displays B−C distances in the range 1.556(8)−1.587(8) Å, comparable to those observed in similar triarylboranes.[10]

Addition of fluoride or cyanide anions to solutions of $[\mathbf{2}]^+$ in acetone resulted in a color change from deep purple to nearly black. To better understand the origin of this color change, we decided to monitor these reactions using UV−vis spectroscopy. The UV−vis spectrum of **2**[OTf] (3.0 mL, 2.5 × 10^{-5} M, THF/DMF, 9/1 vol.) was monitored upon incremental addition of either tetraethylammonium cyanide (TEACN, 3.0 × 10^{-3} M, DMF) or tetrabutylammonium fluoride (TBAF, 3.5 × 10^{-3} M, DMF) (Figure 2). Similar spectral changes were observed for both titrations suggesting a similar mode of interaction of $[\mathbf{2}]^+$ with both fluoride and cyanide (Figure 2). The absorption band at 335 nm, assigned to the absorbance of the triarylborane chromophore, is quenched upon addition of the first equivalent of fluoride or cyanide ions. This phenomenon results from a loss of conjugation in the boron-centered chromophore, indicating formation of **2**-F and **2**-CN (Scheme 2).[18,19] Formation of these complexes is also accompanied by the appearance of a broad band spanning the 360−450 nm range with λ_{max} = 390 nm (ε = 14 200) for both **2**-F and **2**-CN. This behavior is reminiscent of that observed upon addition of fluoride anions to the *N*-methylated pyridinium cation $[\mathbf{1}\text{-Me}]^+$ and is tentatively assigned to a charge transfer transition involving the dimesitylfluoroborate as the donor and the metalated pyridyl ring or 2,2′-bpy ligands as the acceptor.[11] Formation of **2**-F and **2**-CN also results in a bathochromic shift of the Ru(II) $d_\pi \rightarrow$ 2,2′-bpy MLCT band with a shift of the lowest energy edge of the band from 550 to 580 nm. This bathochromic shift can be rationalized by invoking the increased energy and electron-releasing ability of the borylated ligand in **2**-F and **2**-CN (vs $[\mathbf{2}]^+$) leading to a more electron rich Ru(II) center. This explanation is in agreement with the observation that phosphine or 2,2′-bpy ligands decorated by borate units have increased electron-releasing abilities.[20]

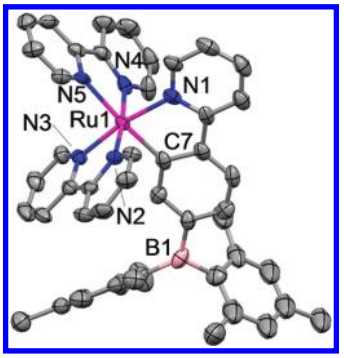

Figure 1. Structure of $[\mathbf{2}]^+$. Displacement ellipsoids are scaled to the 50% probability level. Selected bond lengths (Å) and angles (deg) for **[2]**OTf: Ru(1)−C(7) 2.038(5) Å, Ru(1)−N(1) 2.068(4) Å, Ru(1)−N(2) 2.035(3) Å, Ru(1)−N(3) 2.035(4) Å, Ru(1)−N(4) 2.070(4) Å, Ru(1)−N-(5) 2.152(4) Å; C(7)−Ru(1)−N(1) 79.80(18)°, N(2)−Ru(1)−N(3) 79.24(15)°, N(4)−Ru(1)−N(5) 77.38(15)°, B(1)−C(9) 1.587(8)Å, B-(1)−C(12) 1.556(8) Å, B(1)−C(21) 1.564(8) Å, C(12)−B(1)−C(21) 123.4(5)°, C(12)−B(1)−C(9) 115.4(5)°, C(21)−B(1)−C(9) 121.2(4)°.

The spectral changes induced by fluoride binding to $[\mathbf{2}]^+$ in THF/DMF (9/1 vol.) can be fitted to a 1:1 binding isotherm to provide a fluoride binding constant $K_{(F^-)}$ of 8.0(±2.0) × 10^6 M^{-1} (Figure 2). Encouraged by the magnitude of these

(17) Andres, R.; Brissard, M.; Gruselle, M.; Train, C.; Vaissermann, J.; Malezieux, B.; Jamet, J.-P.; Verdaguer, M. *Inorg. Chem.* **2001**, *40*, 4633–4640. Brissard, M.; Gruselle, M.; Malezieux, B.; Thouvenot, R.; Guyard-Duhayon, C.; Convert, O. *Eur. J. Inorg. Chem.* **2001**, 1745–1751.

(18) Yamaguchi, S.; Akiyama, S.; Tamao, K. *J. Am. Chem. Soc.* **2001**, *123*, 11372–11375.

(19) Solé, S.; Gabbaï, F. P. *Chem. Commun.* **2004**, 1284–1285.

(20) Thomas, C. M.; Peters, J. C. *Organometallics* **2005**, *24*, 5858–5867. Thomas, C. M.; Peters, J. C. *Inorg. Chem.* **2004**, *43*, 8–10.

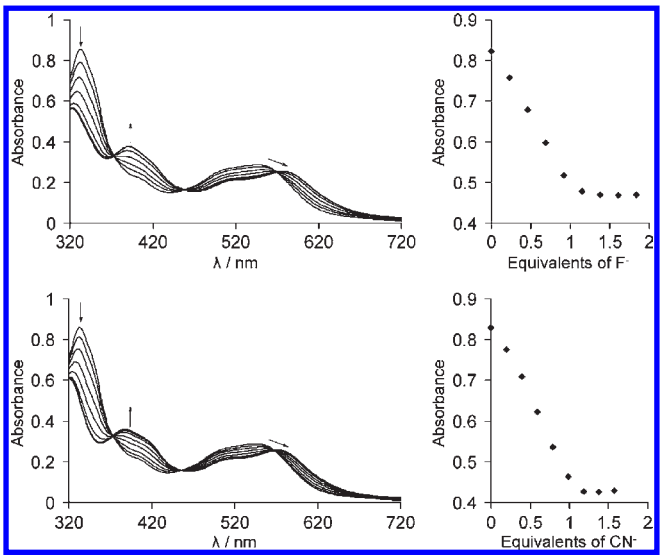

Figure 2. Spectral changes in the UV−vis absorption spectra of [**2**]OTf (2.5×10^{-5} M) in 9/1 DMF/THF upon incremental addition of a TBAF solution (top, 3.5×10^{-3} M in DMF) and TEACN solution (bottom, 3.0×10^{-3} M in DMF). The isotherms are plotted based on the absorbance measured at 338 nm.

Scheme 2

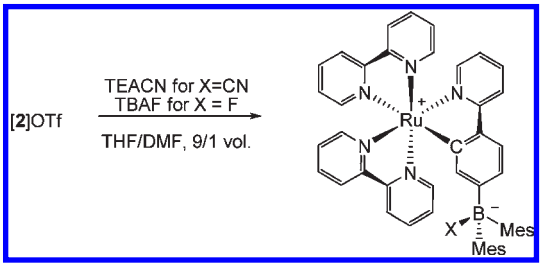

binding constants, we decided to carry out a similar titration in $CHCl_3$/DMF 9/1 vol. The elevated acceptor number of $CHCl_3$[21] (AN = 23.1 for $CHCl_3$ vs 8.9 for THF and 16.0 for DMF) should make such a medium more competitive for anion binding.[22] Accordingly, this experiment afforded a substantially lower $K_{(F^-)}$ of $1.1(\pm0.1) \times 10^4$ M^{-1} (Supporting Information, Figure S2). A lower binding constant $K_{(F^-)}$ of $7.5(\pm0.5) \times 10^2$ M^{-1} was obtained for the free ligand **1** in $CHCl_3$/DMF 9/1 vol. (Supporting Information, Figure S3) thus providing evidence for the beneficial influence of the cationic Ru(II) moiety which increases the anion affinity of the boron center through both inductive and Coulombic effects. The observed fluoride binding constant is, however, notably smaller than the value of $6.5(\pm0.5) \times 10^6$ M^{-1} measured for the phosphonium borane [*p*-($Mes_2B-C_6H_4-PPh_2Me$)]$^+$ in $CHCl_3$.[19] Presumably, the cationic charge of the Ru(II) moiety is largely dissipated on the two 2,2′-bpy ligands leading to a decrease of its inductive influence on the phenylpyridine ligand and boron center. The bulk of the Ru(II) moiety may also hamper the anion-induced tetrahedralization of the boron center.

Next, the affinity of [**2**]$^+$ for cyanide ions was investigated under conditions analogous to those used in the case of fluoride. These experiments afforded $K_{(CN^-)} > 10^7$ M^{-1} in

(21) Mayer, U.; Gutmann, V.; Gerger, W. *Monatsh. Chem.* **1975**, *106*, 1235–1257.

(22) Miyasaka, S.; Kobayashi, J.; Kawashima, T. *Tetrahedron Lett.* **2009**, *50*, 3467–3469.

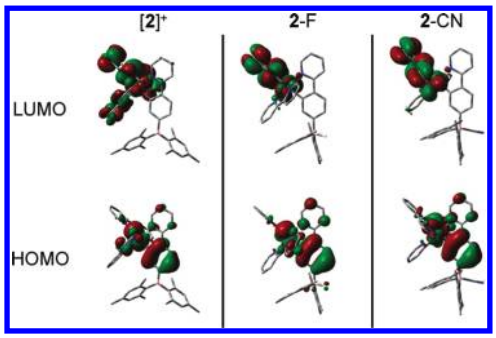

Figure 3. Rendering of the frontier molecular orbitals of [**2**]$^+$ (left), **2**-F (middle), and **2**-CN (right) Isovalues are set at 0.02.

THF/DMF (9/1 vol.) (Figure 2) and $K_{(CN^-)} = 3.0(\pm1.0) \times 10^6$ M^{-1} in $CHCl_3$/DMF 9/1 vol. (Supporting Information, Figure S4) thus indicating that [**2**]$^+$ has a higher affinity for cyanide than fluoride. Reciprocally, these results show that, in these solvent mixtures, the cyanide anion displays a higher basicity toward the boron center of [**2**]$^+$ than fluoride does. Interestingly, this behavior is in agreement with the Brønsted acidity displayed by HCN and HF (pK_a(HCN) = 9.3, pK_a(HF) = 3.18) in water but contrasts with that measured in non-aqueous solvents such as DMSO (pK_a(HCN) = 12.9, pK_a(HF) = 15).[23]

The binding constant measured in $CHCl_3$/DMF 9/1 vol. for [**2**]$^+$ is also significantly higher than that measured for **1** in the same solvent ($K_{(CN^-)} = 4.0(\pm2.0) \times 10^5$ M^{-1}, Supporting Information, Figure S5) once again pointing to the favorable influence of the cationic Ru(II) moiety. Addition of other anions, including Cl^-, Br^-, I^-, or NO_3^- resulted in no changes in the UV−vis spectrum of [**2**]OTf, indicating that these anions do not bind to the boron center. In addition, the reversible nature of fluoride binding to the boron center was confirmed by reappearance of the absorption bands corresponding to [**2**]$^+$ upon addition of a small amount of the fluoride ion scavenger $Al(NO_3)_3$ to solutions of **2**-F (Supporting Information, Figure S6).

The structures of [**2**]$^+$, **2**-F, and **2**-CN have been optimized using DFT methods (B3LYP, Stuttgart RSC 1997 ECP basis set for Ru and 6-31+g(d′) for all other atoms) and subjected to single point energy calculations using the Polarizable Continuum Model (PCM) with THF as a solvent. Inspection of the frontier orbitals shows that the lowest unoccupied molecular orbital (LUMO) is localized on the 2,2′-bpy ligands and a Ru d_π orbital in each of the molecules (Figure 3). It is worth noting that, in the case of [**2**]$^+$, the boron empty p-orbital contributes to the LUMO+2 rather than the LUMO as in typical triarylboranes (Supporting Information, Figure S7). The highest occupied molecular orbital (HOMO) is also similar in each of the three cases, with electron density residing primarily on a Ru d_π orbital and the phenylpyridine ligand. The effects of anion binding are reflected in the marked decrease of the HOMO−LUMO gap going from [**2**]$^+$ (2.78 eV) to **2**-F (2.52 eV) and **2**-CN (2.56 eV) which provides support for the observed redshift in the lowest energy bands of the UV−vis spectrum.

To confirm the formation of **2**-F and **2**-CN, crystallization experiments were undertaken (Figure 4, Table 1). Single

(23) Bordwell, F. G. *Acc. Chem. Res.* **1988**, *21*, 456–463.

crystals of **2**-F were obtained by slow evaporation of a pyridine solution of [**2**]OTf and TBAF at room temperature. The structure of **2**-F confirms the presence of a fluorine atom coordinated to the boron center via a B(1)−F(1) length of 1.468(8) Å, which is comparable to that found in other triarylfluoroborate anions (1.47 Å).[7,18] No significant changes were observed in the Ru(1)−N or Ru(1)−C(7) bond distances when compared to **2**[OTf] (Ru(1)−N, 2.031(5)−2.138(5) Å; Ru(1)−C(7), 2.036(6) Å). Crystals of **2**-CN were obtained by slow evaporation of a CH_3OH/acetone solution containing KCN and **2**[OTf]. The structure clearly displays a cyanide anion bound to the boron center with a B(1)−C(50) distance of 1.635(8) Å. While the Ru(1)−N bond distances in **2**-CN (Ru(1)−N, 2.033(4)−2.141 (4) Å) again experience no significant changes versus **2**[OTf] or **2**-F, the Ru(1)−C(7) bond length is slightly elongated (2.062(5) Å), possibly resulting from increased ligand steric repulsion caused by pyramidalization of the boron center.

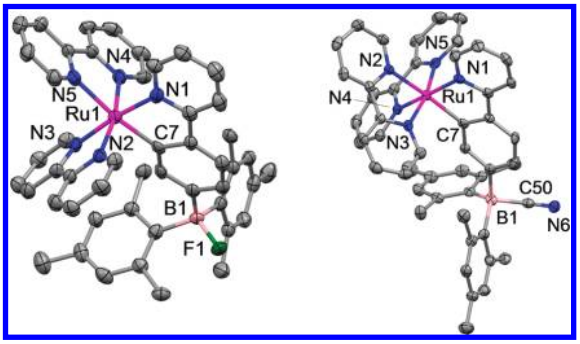

Figure 4. Structure of **2**-F (left) and **2**-CN (right). Displacement ellipsoids are scaled to the 50% probability level. Interstitial solvent molecules and hydrogen atoms omitted for clarity. Selected bond lengths (Å) and angles (deg) for: **2**-F: Ru(1)−C(7) 2.036(6), Ru(1)−N(1) 2.068(5), Ru(1)−N(2) 2.031(5), Ru(1)−N(3) 2.043(5), Ru(1)−N(4) 2.055(5), Ru(1)−N(5) 2.138(5); C(7)−Ru(1)−N(1) 79.6(2), N(2)−Ru(1)−N(3) 78.65(19), N(4)−Ru(1)−N(5) 77.76(19), B(1)−F(1) 1.468(8), B(1)−C(9) 1.651(10), B(1)−C(12) 1.652(10), B(1)−C(21) 1.675(9), F(1)−B(1)−C(9) 103.6(5), F(1)−B(1)−C(12) 111.4(5), C(9)−B(1)−C(12) 109.4(5), F(1)−B(1)−C(21) 102.9(5), C(9)−B(1)−C(21) 119.0(5), C(12)−B(1)−C(21) 110.1(5). **2**-CN: Ru(1)−C(7) 2.062(5), Ru(1)−N(1) 2.076(4), Ru(1)−N(2) 2.141(4), Ru(1)−N(3) 2.063(4), Ru(1)−N(4) 2.053(4), Ru(1)−N(5) 2.033(4); C(7)−Ru(1)−N(1) 80.08(17), N(2)−Ru(1)−N(3) 76.89(16), N(4)−Ru(1)−N(5) 78.33(17), B(1)−C(50) 1.635(8), B(1)−C(9) 1.648(7), B(1)−C(12) 1.659(7), B(1)−C(21) 1.675(7), C(9)−B(1)−C(12) 108.3(4), C(9)−B(1)−C(21) 118.9(4), C(12)−B(1)−C(21) 112.0(4), C(50)−B(1)−C(9) 103.2(4), C(50)−B(1)−C(12) 114.6(4), C(50)−B(1)−C(21) 99.4(4).

The formation of **2**-F and **2**-CN was also studied by ^{1}H NMR. Addition of TBAF to a solution of **2**[OTf] in acetone-d_6 resulted in the appearance of a new set of ^{1}H NMR signals assigned to **2**-F. Significant broadening of many of the signals in the ^{1}H NMR spectrum of **2**-F suggests restricted molecular motion caused by pyramidalization of the boron atom. Nonetheless, addition of $Al(NO_3)_3$ to the NMR sample leads to a revival of the original purple color, as well as of the sharp resonances assigned to $[\mathbf{2}]^+$ thus supporting formation of **2**-F. Despite extended acquisition times, the ^{11}B NMR signal of **2**-F could not be detected. Its ^{19}F NMR spectrum is dominated by a resonance at −174 ppm appearing in the expected range for a fluoroborate species. The ^{1}H NMR spectrum of **2**-CN displays two distinct sets of Mes-C*H* signals at 6.64 and 6.75 ppm as well as two *ortho*-Mes-CH_3 (2.14 and 2.45 ppm) and *para*-Mes-CH_3 (2.24 and 2.29 ppm) resonances, in agreement with the diastereotopic relationship of the two mesityl groups. The^{11}B NMR spectrum of **2**-CN displays a sharp signal at −12.7 ppm, in the typical range for a triaryl cyanoborate.[3−5]

Encouraged by the high affinity that $[\mathbf{2}]^+$ displays for cyanide and fluoride, we decided to determine if the readily accessible $Ru^{II/III}$ redox couple could be used to report anion binding events occurring at the boron center. To this end, we

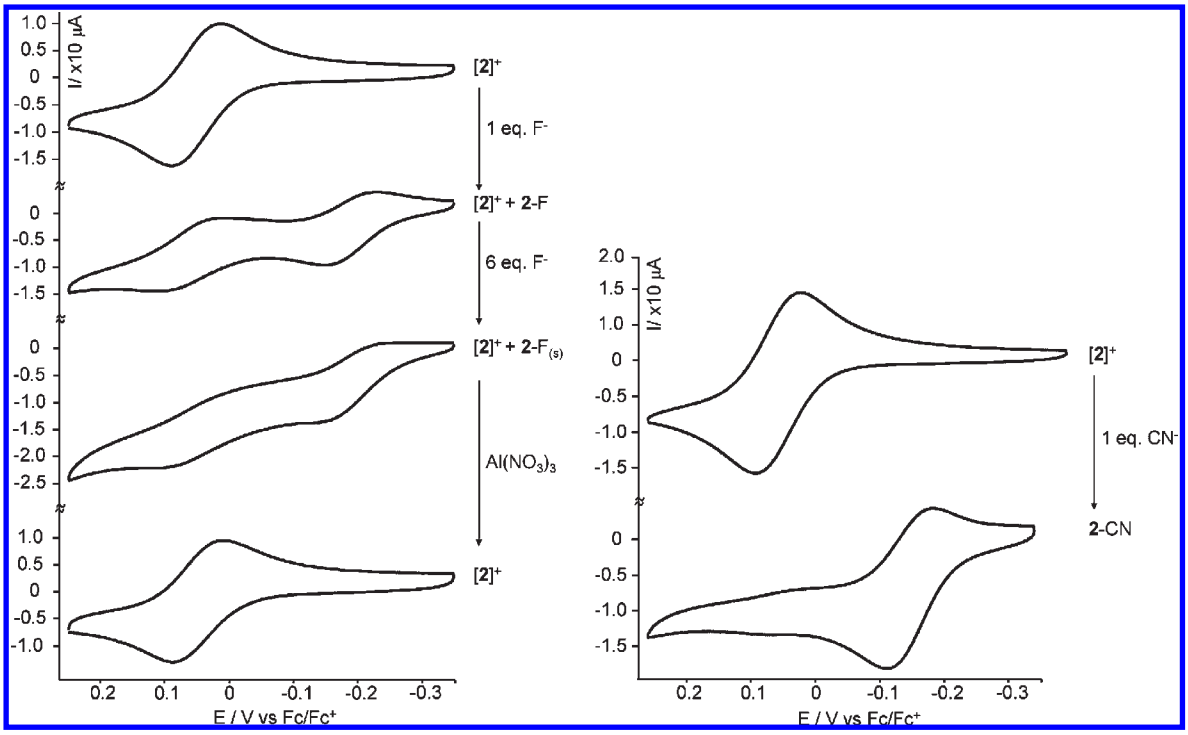

Figure 5. Cyclic voltammograms of [**2**]OTf and in situ generated **2**-F (left), and **2**-CN (right) in DMF ([[**2**]OTf] = 1 mM, [n−Bu_4PF_6] = 0.1 M ν = 200 mV s^{-1}).

first recorded the cyclic voltammogram of $[\mathbf{2}]^+$ (1 mM, 0.1 M $TBAPF_6$, DMF) which displays a reversible oxidation wave for the $Ru^{II/III}$ redox couple at $E_{1/2} = 0.051$ V versus Fc/Fc^+. Addition of 1 equiv of TBAF to $[\mathbf{2}]^+$ in the electrochemical cell resulted in the appearance of a new wave at $E_{1/2} = -0.191$ V versus Fc/Fc^+ assigned to the presence of **2**-F (Figure 5). This cathodic shift of the $Ru^{II/III}$ redox process is in agreement with an increase in the donor strength of the cyclometallating ligand induced by anion binding[20] and a decrease in the overall charge of the complex. Appearance of the new wave at $E_{1/2} = -0.191$ V was accompanied by a decrease in the intensity of the oxidation wave of $[\mathbf{2}]^+$ (Figure 5). Increasing the fluoride ion concentration resulted in a net decrease of both oxidation waves corresponding to $[\mathbf{2}]^+$ and **2**-F. This unexpected phenomenon is assigned to further conversion of $[\mathbf{2}]^+$ to **2**-F and subsequent precipitation of the latter at higher fluoride concentration. In agreement with this interpretation, addition of the fluoride ion scavenger $Al(NO_3)_3$ to the electrochemical cell led to the nearly full reappearance of the oxidation wave at $E_{1/2} = +0.051$ V versus Fc/Fc^+, indicating regeneration of the cationic species $[\mathbf{2}]^+$. Addition of cyanide ions to a solution of $[\mathbf{2}]^+$ in the electrochemical cell triggered formation of **2**-CN as evidenced by the detection of an new oxidation wave at $E_{1/2} = -0.147$ V versus Fc/Fc^+. Conversion of $[\mathbf{2}]^+$ into **2**-CN was not complicated by precipitation; moreover, the conversion appeared quantitative, in agreement with the elevated cyanide binding constant displayed by $[\mathbf{2}]^+$.

Conclusion

In conclusion, we report a cationic cyclometalated ruthenium(II) complex ($[\mathbf{2}]^+$) decorated by a peripheral Lewis acidic boryl moiety. This new complex reacts with fluoride and cyanide anions to afford the corresponding zwitterionic fluoroborate and cyanoborate species. The elevated stability constants of these new species indicate that the cationic transition metal moiety increases the Lewis acidity of the boron center via inductive and Coulombic effects. The cyanide binding constant of $[\mathbf{2}]^+$ is elevated thus suggesting that such compounds could be used to monitor very low concentrations of this anion. Lastly, anion binding to the boron center affects the photophysical and electrochemical properties of the ruthenium center which can be used to monitor anion binding. Most notably, the potential of the $Ru^{II/III}$ couple experiences a cathodic shift upon anion binding making such compounds attractive for electrochemical sensing applications.

Acknowledgment. This work was supported by the National Science Foundation (CHE-0646916 and CHE-0541587), the Welch Foundation (Grant A-1423), and the U.S. Army Medical Research Institute of Chemical Defense.

Supporting Information Available: Optimized geometries of $[\mathbf{4}]^+$, **2**-F, and **2**-CN. UV−vis titration data in $CHCl_3$, X-ray crystallographic data in CIF format. This material is available free of charge via the Internet at http://pubs.acs.org.